

HCN (1-0) opacity of outflowing gas in Arp 220W

J. Z. Wang^{1,2}, S. Liu^{3,4}, Z.-Y. Zhang^{5,6}, and Y. Shi^{5,6}

¹ Shanghai Astronomical Observatory, Chinese Academy of Sciences, 80 Nandan Road, Shanghai, 200030, PR China
e-mail: jzwang@shao.ac.cn

² Key Laboratory of Radio Astronomy, Chinese Academy of Sciences, 10 Yuanhua Road, Nanjing, Jiangsu 210033, PR China

³ National Astronomical Observatories, Chinese Academy of Sciences, Beijing 100012, PR China
e-mail: liushu@nao.cas.cn

⁴ CAS Key Laboratory of FAST, National Astronomical Observatories, Chinese Academy of Sciences, Beijing 100012, PR China

⁵ School of Astronomy and Space Science, Nanjing University, Nanjing, 210093, PR China

⁶ Key Laboratory of Modern Astronomy and Astrophysics (Nanjing University), Ministry of Education, Nanjing 210093, PR China

Received xx / accepted xx

ABSTRACT

Context. We present our findings for the HCN/H¹³CN 1-0 line ratio in the molecular outflow of Arp 220 west based on high-resolution ALMA data.

Aims. Molecular gas masses in the outflowing gas of galaxies driven by active galactic nuclei (AGNs) or starbursts are important parameters for understanding the feedback of these latter two phenomena and star-formation quenching. The conversion factor of line luminosities to masses is related to the optical depth of the molecular lines.

Methods. Using H¹³CN 1-0, the isotopic line of HCN 1-0, to obtain the line ratio of HCN/H¹³CN 1-0 is an ideal way to derive the optical depth of HCN 1-0 in outflowing gas.

Results. With the nondetection of H¹³CN 1-0 in the outflowing gas, a 3σ lower limit of HCN/H¹³CN 1-0 line ratio is obtained, which is at least three times higher than that found in the whole of the whole system of Arp 220. The high HCN/H¹³CN 1-0 line ratio indicates low opacity of HCN 1-0 in the outflowing gas, even though the upper limit of HCN 1-0 opacity obtained here is still not good enough to draw any robust conclusions if HCN 1-0 is optically thin. A lower conversion factor of HCN 1-0 luminosity to dense gas mass in the outflowing gas should be used than that used for the host galaxy of Arp 220.

Key words. opacity – galaxies: individual: Arp 220 – methods: data analysis

1. Introduction

Mass outflows, a major manifestation of the feedback from active galactic nuclei (AGNs) and circumnuclear extreme starbursts (SBs), is one key element for understanding galaxy evolution (Feruglio et al. 2010; Sturm et al. 2011). Massive molecular outflows driven by AGNs or SBs have been found in galaxies with CO emissions (Feruglio et al. 2010; Cicone et al. 2012, 2014; Fluetsch et al. 2019) and far infrared OH absorption lines (Fischer et al. 2010). Outflow rates of molecular gas in starburst-dominated galaxies have been found to be comparable to or even higher than their star formation rates (Cicone et al. 2014; Fluetsch et al. 2019). Furthermore, it has been suggested that a high-mass outflow rate can effectively quench star formation, which may cause the host galaxy to quickly leave the star-forming phase to become an early-type gas-poor red galaxy.

Such outflows can also be detected with dense gas tracers. Examples are HCN, HCO⁺, and HNC lines in Mrk 231 (Aalto et al. 2012, 2015), HCN 1-0 in Arp 220 (Barcos-Muñoz et al. 2018), and HCO⁺ and HCN 1-0 in NGC 3256 (Michiyama et al. 2018). The mass-loss rate and outflow mass can be estimated with line luminosities of HCN and HCO⁺ wings. However, such estimations strongly depend on the conversion factor from line luminosity to dense gas mass, which is related to the relative abundance of HCN and HCO⁺ to hydrogen and the line opacity. The conversion factor of $\alpha_{\text{HCN}(1-0)} = 3.3 M_{\odot} (\text{K km s}^{-1} \text{pc}^2)^{-1}$

whilst the optically thick assumption has been used to estimate the upper limit of the mass of the dense molecular outflow in Mrk 231 (Aalto et al. 2015), while $\alpha_{\text{HCN}(1-0)}$ is $0.24 M_{\odot} (\text{K km s}^{-1} \text{pc}^2)^{-1}$, if the optically thin assumption is made (Barcos-Muñoz et al. 2018). On the other hand, Michiyama et al. (2018) used 0.24 and $10 M_{\odot} (\text{K km s}^{-1} \text{pc}^2)^{-1}$ to calculate the lower and upper limit of dense gas mass in NGC 3256. Isotopologue lines of HCN and HCO⁺ molecules, such as H¹³CN and H¹³CO⁺ lines, can be used to determine the opacities of HCN and HCO⁺ lines with line ratios of HCN/H¹³CN and HCO⁺/H¹³CO⁺, and were adopted to obtain averaged HCN opacities in nearby galaxies (Wang et al. 2016; Li et al. 2020).

Arp 220, as the nearest ultraluminous infrared galaxy (ULIRG) in the late stages of a galaxy merger, with strong outflowing gas at about $\pm 400 \text{ km s}^{-1}$ and more than $10^7 M_{\odot}$ mass around the western nucleus (Arp 220W) detected with HCN 1-0 (Barcos-Muñoz et al. 2018), is a good candidate to determine the line ratio of HCN/H¹³CN 1-0 for the outflowing gas, which can be used to determine the opacity of HCN 1-0 in outflowing gas.

In this letter, we describe the data from the ALMA archive. First we present our data reduction in §2, before presenting our main results in §3, and discussions in §4. We provide a brief summary in §5.

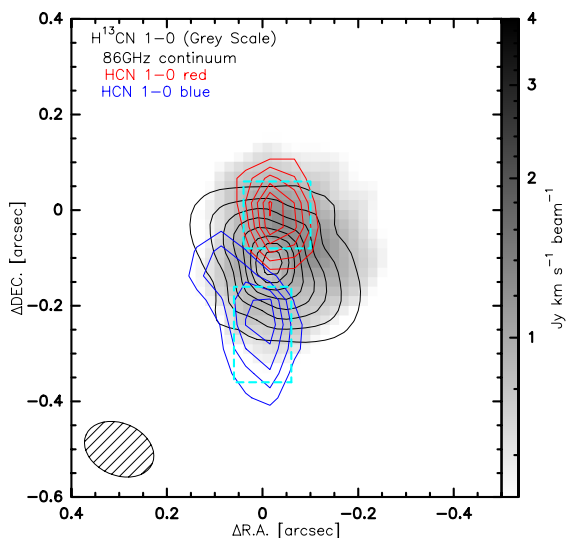


Fig. 1: The 86 GHz continuum (black contour with levels starting from 3 mJy beam^{-1} in steps of 1 mJy beam^{-1}), a velocity integrated map of H^{13}CN 1-0 (grey scale, in units of $\text{Jy km s}^{-1}\text{ beam}^{-1}$), a velocity integrated map of HCN 1-0 red wing (red contour with levels starting from $0.2\text{ Jy km s}^{-1}\text{ beam}^{-1}$ in steps of $0.05\text{ Jy km s}^{-1}\text{ beam}^{-1}$) and a velocity integrated map of HCN 1-0 blue wing (blue contour with levels starting from $0.2\text{ Jy km s}^{-1}\text{ beam}^{-1}$ in steps of $0.05\text{ Jy km s}^{-1}\text{ beam}^{-1}$), around the centre of Arp 220 west. The dashed cyan boxes are the regions for the spectra in Figures 2 and 3. The restoring beam ($0.151'' \times 0.109''$, $PA = 23.4^\circ$) of the data cube is shown in the bottom left. The central coordinates of this map are R.A.: 15:34:57.22 and Dec: 23:30:11.6 (J2000).

2. The data

The data were taken from the ALMA archival system (project number: 2015.1.00702.S, PI: L. Barcos-Muñoz), the same data set used in Barcos-Muñoz et al. (2018). Standard bandpass, phase, and flux calibrations using scripts from the archive system were done in CASA, as well as imaging and deconvolution using natural weighting with a pixel size of $0.02''$ and frequency resolution of 3.906 MHz in the task ‘tclean’. The continuum image obtained from line-free channels, the velocity-integrated maps of HCN 1-0 at the rest frequency of 88.6318473 GHz for both red and blue wings, as well as the velocity integrated maps of the optically thin isotopologue H^{13}CN 1-0, were obtained from the cleaned datacube (see Figure 1). Spectra of HCN and H^{13}CN 1-0 at the rest frequency of 86.3401764 GHz toward red and blue wings from the regions marked as dashed cyan boxes in Figure 1 were also obtained and are presented in Figures 2 and 3.

3. Results

3.1. Spatial distribution of outflow traced by HCN

The velocity-integrated flux distribution of the red and blue wings of HCN 1-0, as well as the continuum emission around 86 GHz and the velocity-integrated flux of H^{13}CN 1-0 near the centre of Arp 220W are presented in Figure 1. Outflows near the centre of Arp 220W can be seen with HCN 1-0 emission, which is consistent with the findings reported by Barcos-Muñoz et al. (2018), with a blue wing at the northern side and a red wing at the southern side of the centre of Arp 220W traced by continuum emission. As the abundance of H^{13}CN is less than one-

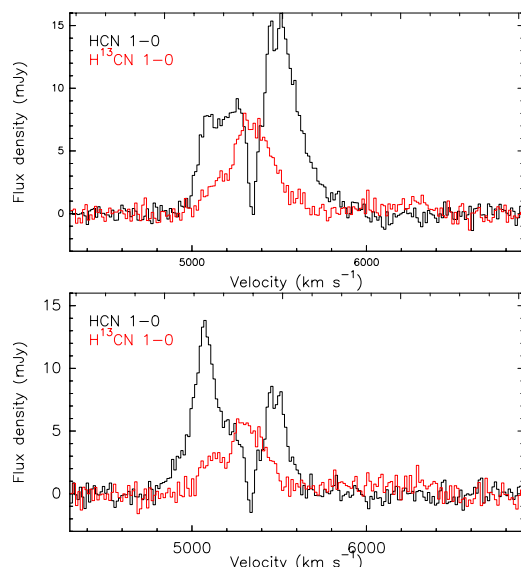


Fig. 2: Top: HCN (black) and H^{13}CN 1-0 (red) spectra collected from the red wing region of the cyan box in Figure 1. Bottom: Same as the top spectra but from the blue wing region. Radio-defined velocities are used, while the system velocity is about 5350 km s^{-1} .

tenth of HCN, H^{13}CN 1-0 is normally optically thin in Galactic star forming regions (Padovani et al. 2011; Colzi et al. 2018) and galaxies (Henkel et al. 1998; Li et al. 2020). However, H^{13}CN 1-0 in Arp 220W shows an offset of the peak emission from that of the continuum, obtained from (see Figure 1). Such an offset may be caused by absorption of H^{13}CN 1-0 towards continuum emission around the centre region, where the absorption of HCN 1-0 is significantly below the continuum level at some velocity ranges. HCN 1-0 absorption can be important even at the positions with less continuum emission than the centre (see Figure 2 and 3).

Collecting the most significant emitting regions of red and blue wings marked as dashed cyan boxes in Figure 1, HCN and H^{13}CN 1-0 spectra are obtained to determine the line ratios of HCN/ H^{13}CN 1-0 in the line wings. The red wing displayed in Figure 1 shown with red contours is integrated from 5620 to 5800 km s^{-1} as radio-defined velocity, while the blue wing shown with blue contours is integrated from 4860 to 5040 km s^{-1} . The SO line at the rest frequency of 86.093983 GHz and HC^{15}N 1-0 at the rest frequency of 86.054967 GHz can contaminate the red wing of H^{13}CN 1-0 (see Figure 3), especially with velocity higher than 6000 km s^{-1} . Therefore, in order to avoid such contaminations when estimating the HCN/ H^{13}CN 1-0 ratio, even though there are no such contaminations for the HCN 1-0 line, only the velocity range between 5620 and 5800 km s^{-1} is integrated for the red wing.

3.2. HCN/ H^{13}CN 1-0 line ratio

The HCN 1-0 emission is no more than five times the corresponding H^{13}CN 1-0 emission in most of the velocity components towards the red and blue wings of the outflowing gas (see Figure 3). The HCN/ H^{13}CN 1-0 ratio in the entire system of Arp 220 is about five according to single-dish observations with IRAM 30-meter telescope (Wang et al. 2016). HCN and H^{13}CN 1-0 fluxes measured from ALMA data are consistent with those obtained with the IRAM 30-meter telescope (Wang

et al. 2016). HCN/H¹³CN 1-0 ratios towards the outflowing regions vary along with different velocities (see Figure 2 and 3), from more than five to even less than one at the line centre, which seems likely to be caused by the absorption of HCN 1-0 towards continuum emission or the self absorption of HCN 1-0 with a temperature gradient. Such an absorption, where the velocity of the HCN 1-0 absorption peak is similar to that of the H¹³CN 1-0 emission peak, will cause an overestimation of opacity if a unique temperature is assumed for the molecular gas. However, such absorption is mainly caused by gas from the disc instead of the outflowing gas, based on the velocity information.

The line profile of HCN 1-0 from the red wing region (see Figure 3) in the blue part from about 4950 to 5100 km s⁻¹ agrees well with the spectra of H¹³CN 1-0 from the same region, with a line ratio of about five. On the other hand, the intensity of HCN 1-0 is well above five times that of H¹³CN 1-0 at the red part, especially from 5620 to 5800 km s⁻¹. The SO line at the rest frequency of 86.093983 GHz contaminates H¹³CN 1-0 from ~5850 km s⁻¹ to 6100 km s⁻¹. Thus, it is hard to obtain a reliable ratio of HCN and H¹³CN 1-0 at velocity ranges with SO line contamination. SO and HC¹⁵N 1-0 emission can also be seen in the blue wing regions (See Figure 3). However, the line profiles of HCN and H¹³CN 1-0 from the blue wing region agree well with each other in the red part without SO contamination, with a line ratio also similar to five, while HCN 1-0 intensity is well above five times that of H¹³CN 1-0 in the blue region (see Figure 3). In summary, HCN 1-0 emission is significantly above five times that of H¹³CN 1-0 from the outflowing gas, while it is equal to or below five times that of the H¹³CN 1-0 emission from the gas that is not outflowing.

The HCN 1-0 velocity-integrated flux of the red wing in Figures 2 and 3 between 5620 and 5800 km s⁻¹ is 631.1±22.5 mJy km s⁻¹, while this value is 794.1±27.7 mJy km s⁻¹ for the blue wing between 4860 and 5040 km s⁻¹ (see Table 1). The uncertainties are estimated with $\sigma_{rms} \times \sqrt{\delta v \Delta V}$, where σ_{rms} is the rms with baseline fitting for the spectra shown in Figure 2 at the velocity resolution of δv as ~13.2 km s⁻¹, while ΔV is 180 km s⁻¹ which is the integrated line width for both red and blue wings. The velocity-integrated fluxes of H¹³CN 1-0 at the corresponding velocities are 59.7 and 61.5 mJy km s⁻¹ for the red and blue wings, respectively, which is below the 3 σ level for both components. The noise level near H¹³CN 1-0 is about 0.94 of that of the HCN 1-0 line. Thus, the 3 σ values 63.2 and 77.9 mJy km s⁻¹ are used for the red and blue wings, respectively, which give line ratios of HCN/H¹³CN 1-0 greater than 9.5 and 9.7 in the red and blue wings, after converting the units from mJy for flux density to mK for brightness temperature.

The line ratio HCN/H¹³CN 1-0 varies from 7.6±2.8 in NGC 4418 to 40±3.6 in M82 within a sample of local galaxies (Li et al. 2020). Thus, the high HCN/H¹³CN 1-0 ratio of greater than 9.6 in the line wings of Arp 220W is not extremely high in galaxies. On the other hand, the HCN/H¹³CN 1-0 line ratio of about five for the whole galaxy of Arp 220 (Wang et al. 2016) indicates that HCN column density in Arp 220 is extremely high, which is consistent with our knowledge of Arp 220 as a gas-rich late-stage merger with extreme starburst activity.

4. Discussion

4.1. HCN 1-0 opacity in the outflowing gas

The average line ratio of HCN/H¹³CN 1-0 in Arp 220 is about five based on single-dish observations (Wang et al. 2016), which gives an average opacity of ~22 for HCN 1-0, assuming the

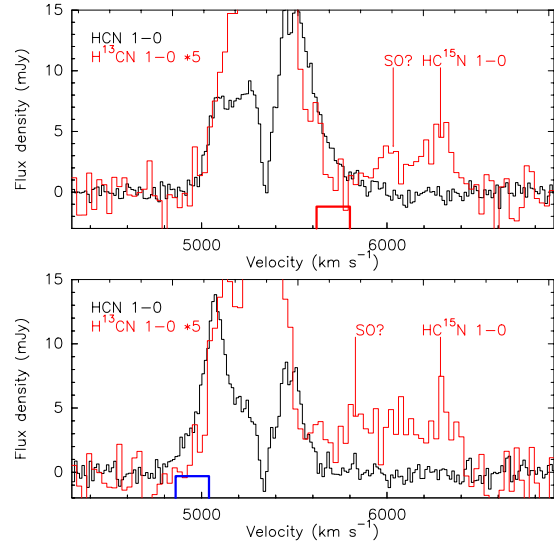


Fig. 3: As in Figure 2, but with H¹³CN 1-0 multiplied by 5. The red window in the top panel is for the velocity range from 5620 to 5800 km s⁻¹ which integrates the red wing of the outflow in Figure 1, while the blue window in the bottom panel is for the blue wing from 4860 to 5040 km s⁻¹.

abundance ratio ($X_{\text{HCN}}/X_{\text{H}^{13}\text{CN}}$) is the same as the ¹²C/¹³C ratio, namely 100, which was suggested by Martín et al. (2011) based on observations of ¹³CO/C¹⁸O 2-1. The optical depth is obtained with $\frac{I_{\text{H}^{13}\text{CN}1-0}}{I_{\text{HCN}1-0}} = \frac{1 - e^{-\tau(\text{H}^{13}\text{CN}1-0)}}{1 - e^{-\tau(\text{HCN}1-0)}}$, where $\frac{I_{\text{H}^{13}\text{CN}1-0}}{I_{\text{HCN}1-0}}$ is the measured line ratio, while $\frac{\tau(\text{H}^{13}\text{CN}1-0)}{\tau(\text{HCN}1-0)}$ is assumed to be the same as the abundance ratio of ¹³C/¹²C. By adopting a HCN/H¹³CN 1-0 ratio of five, the line profile of H¹³CN is close to that of HCN in the velocity ranges of 5000-5100 km s⁻¹ (Figure 3 top) and 5500-5600 km s⁻¹ (Figure 3 bottom). This illustrates that there are no strong contaminations from HCN 1-0 absorption in the two velocity ranges, and that these ranges are not affected by outflowing gas in the regions with red and blue wings near Arp 220W. For the emissions near the central regions of both Arp 220 west and east, absorption of both HCN 1-0 and H¹³CN 1-0 cannot be neglected, which poses a problem for estimating opacity of HCN 1-0 there. Absorption of HCN 1-0 towards the continuum emission or HCN 1-0 emission from inner warm dense molecular gas can result in overestimation of the opacity of HCN 1-0 because of the underestimation of HCN 1-0 emission.

The line ratios of HCN/H¹³CN 1-0 in the red and blue wings are greater than 9.5 and 9.7, respectively, giving a 3 σ upper limit of ~0.1 for the opacity of H¹³CN 1-0 in the outflowing gas. Assuming an $X_{\text{HCN}}/X_{\text{H}^{13}\text{CN}}$ abundance ratio of 100 as suggested by Martín et al. (2011) with the ¹³CO/C¹⁸O 2-1 line ratio obtained with the Submillimeter Array (SMA), the opacity of HCN 1-0 should be less than 10.5.

The HCN 1-0 flux combined between 5620 and 5800 km s⁻¹ in the red wing and between 4860 and 5040 km s⁻¹ in the blue wing integrated within the dashed cyan boxes in Figure 1 is 1425.2±35.7 mJy km s⁻¹, where the flux is from the sum of HCN 1-0 flux from the red wing of 631.1 mJy km s⁻¹, and that from the blue wing of 794.1 mJy km s⁻¹, while the noise level is $\sqrt{22.5^2 + 27.7^2}$ mJy km s⁻¹. The corresponding H¹³CN 1-0 flux is 121.3±35.7 mJy km s⁻¹ derived in the same way, that is, 59.7+61.5 mJy km s⁻¹ with noise of $\sqrt{21.1^2 + 25.9^2}$ mJy km s⁻¹. In other words, H¹³CN 1-0 emission is about 3.4 σ . How-

Table 1: HCN 1-0 and H¹³CN 1-0 in the outflows of Arp 220W

Line	Integrated flux mJy km s ⁻¹	Optical depth
HCN 1-0 (blue)	794.1±27.7	<4.4
H ¹³ CN 1-0 (blue)	<83.9 (3σ)	<0.11
HCN 1-0 (red)	631.1±22.5	<4.4
H ¹³ CN 1-0 (red)	<67.5 (3σ)	<0.11

Note. The optical depth of HCN 1-0 is estimated with a ¹²C/¹³C ratio of 40 (Wheeler et al. 2020).

ever, as the low-velocity components are included, which may be mainly from the disc instead of outflowing gas, the H¹³CN 1-0 emission contribution should be mainly from optically thick non-outflowing gas. Thus, the non-detection of H¹³CN 1-0 emission from the outflowing gas should still be considered and a 3σ upper limit should be used for estimating the line ratio of HCN/H¹³CN 1-0 for the combined regions of outflowing gas, which gives a ratio of greater than 13.3 and an opacity of H¹³CN 1-0 of less than 0.078, or less than 0.11 for both the red and blue wings if calculating them individually. Assuming the HCN/H¹³CN abundance ratio of 100 as suggested by Martín et al. (2011), the opacity of HCN 1-0 should be less than 7.8, which is about one-third of the average value in Arp 220. Thus, even though we do not have enough information to derive the opacity of HCN 1-0 in the outflowing gas, the upper limit on HCN 1-0 opacity in the outflowing gas is less than one-third of the average value in Arp 220.

The ¹²C/¹³C ratio in Arp 220 was updated to be 40 with ALMA observations of ¹²CO 3-2 and ¹³CO 4-3 (Wheeler et al. 2020). Therefore, the opacity of HCN 1-0 should be about 40% of the opacity estimated using the ¹²C/¹³C ratio of 100 suggested by Martín et al. (2011), both of which are less than 4.4 as listed in Table 1. Even with a 3σ upper limit of HCN 1-0 opacity in the outflowing gas combined for the red and blue components of 3.1, it is still not possible to draw a firm conclusion as to whether HCN 1-0 is optically thin or thick in the outflowing gas of Arp 220. The average opacity of HCN 1-0 in the whole galaxy is down to ~9 using the updated ¹²C/¹³C in Arp 220 (Wheeler et al. 2020). The optical depth of HCN 1-0 in the outflowing gas is at least three times less than that in the host galaxy of Arp 220 if the same HCN/H¹³CN abundance ratio is used. However, the possibility of higher HCN/H¹³CN abundance ratio in the outflowing gas than that in the galaxy can also enhance the HCN/H¹³CN 1-0 line ratio, even though it is not likely to lead to significantly different line ratios between the outflowing gas and the gas in the whole galaxy. In summary, even though we can conclude that the optical depth of HCN 1-0 in the outflowing gas is at least a factor of three lower than the average value for the whole galaxy, whether HCN 1-0 is optically thick or thin remains uncertain.

4.2. Outflow properties and future prospects

Therefore, even though the accurate opacity of HCN 1-0 of the outflowing gas in Arp 220W cannot be determined because of the limited sensitivity of the observations, the non-detection of H¹³CN 1-0 from the outflowing gas provides a good lower limit on the HCN/H¹³CN 1-0 line ratio there. Based on this ratio, an upper limit on the HCN 1-0 opacity of less than one-third of the average value over the whole of Arp 220 can be obtained. It is necessary to use a smaller conversion factor of HCN 1-0 luminosity to dense gas mass than that used for normal galaxies, namely of 10 M_⊙ (K km s⁻¹ pc²)⁻¹ (Michiyama et al. 2018). The

conversion factor under optically thin conditions, namely 0.24 M_⊙ (K km s⁻¹ pc²)⁻¹, was used to estimate the lower limit of outflowing mass and mass loss rate in Arp 220W (Barcos-Muñoz et al. 2018). The CO 1-0 luminosity of the outflowing gas in Arp 220W is similar to that of HCN 1-0 (Barcos-Muñoz et al. 2018), which means an even higher HCN/CO 1-0 luminosity ratio than that in the massive outflowing gas from the central AGN in Mrk 231 (Aalto et al. 2012). If the same conversion factor of line luminosity to mass ratio is used in Arp 220W and Mrk 231, the dense gas fraction in the outflowing gas in Arp 220W is higher than that in Mrk 231, and even the outflowing gas in Mrk 231 is more massive than that in Arp 220W.

However, such conversion factors strongly depend on the opacity of CO and HCN lines, as well as HCN and CO abundances in the outflowing gas. The abundance issue of HCN when determining dense gas, which can cause uncertainties of estimating the dense gas mass, can be done with lines of different molecules with high dipole moments, such as HCN, HCO⁺, HNC, and CS. With observations of different lines of similar critical density, the effect of chemical enhancement of special molecules, such as HCN or HCO⁺, can be found, as discussed for the outflowing gas in Mrk 231 (Lindberg et al. 2016). The outflowing gas traced by HCO⁺ 1-0 shows similar distribution to that of HCN 1-0 in Arp 220W, with the same dataset (Barcos-Muñoz 2016), which indicates that astrochemical enhancement of the abundance of the HCN molecule is not significant in the outflowing gas. However, new observations of HNC 1-0 and CS 2-1 are required to further confirm such abundance effects.

The opacity of lines in the outflowing gas can be determined from observations of their optically thin isotopologues, such as H¹³CN 1-0 for HCN 1-0. The data used in this work were obtained from observations lasting about 1.9 hours on source with ALMA. If H¹³CN 1-0 data of three times higher sensitivity are required to obtain the 3σ upper limit of HCN 1-0 opacity of about 1 with a ¹²C/¹³C ratio of approximately 40 measured with ALMA (Wheeler et al. 2020), the required total telescope time would be about 20 hours; including overheads, this would be prohibitively expensive. Using the RADEX online calculator (van der Tak et al. 2007), when HCN molecules are close to local thermal equilibrium (LTE), the opacity of HCN 2-1 is about 3.5 times that of HCN 1-0 under optically thin conditions. Therefore, it would be more effective to derive the opacity of HCN 2-1 with observations of HCN and H¹³CN 2-1 than that of HCN 1-0. H¹³CN 2-1 in the outflowing gas in Arp 220W can be expected to be detected within several hours using ALMA, because HCN 2-1 has moderate opacity of around 0.5 to 1.0, even though HCN 1-0 is optically thin. Otherwise, an upper limit on HCN 2-1 opacity of approximately 0.5 would also be useful to determine whether or not HCN 1-0 is optically thin. Stronger HCN 2-1 emission than that of 1-0 was also found in the outflowing gas of Mrk 231 (Lindberg et al. 2016) without significant line contamination of HCN 2-1. On the other hand, there is one strong line within ±700 km s⁻¹ range of H¹³CN 2-1, namely HC₃N 19-18 at 172.849287GHz at a velocity of ~300 km s⁻¹ relative to H¹³CN 2-1 at 172.67796GHz. Because of the relatively low abundance ratio of HC₃N to HCN and the high density and temperature requirement for the excitation of J=19, contamination of HC₃N 19-18 at the outflowing region can be neglected.

Deep ¹³CO 2-1 and 1-0 observations may also be useful for determining the opacities of CO 1-0 and 2-1 in Arp 220W. However, because the line luminosity of CO 1-0 is comparable to that of HCN 1-0, there is no great advantage to using ¹³CO lines instead of H¹³CN. Combining ¹³CO 2-1 and CO 2-1 data with those for HCN 2-1 and H¹³CN 2-1 may be a good choice for de-

termining whether CO and HCN lines in the outflowing gas are optically thick or thin. H^{13}CN or ^{13}CO lines towards local massive AGN molecular outflows or other extreme starbursts with strong outflow, such as NGC 3256 (Michiyama et al. 2018) or M82 (Chisholm & Matsushita 2016), will be helpful for understanding such outflows.

5. Summary

We present an ideal method to derive optical depths of HCN 1-0 in Arp 220 using the HCN/ H^{13}CN line ratios. We apply this method to the outflowing gas of galaxies and use it to better determine the conversion factor from line luminosity to mass. With information from spatially resolved H^{13}CN 1-0 and HCN 1-0 observations in Arp 220 with ALMA, we obtain a 3σ lower limit on the HCN/ H^{13}CN 1-0 line ratio in the outflowing gas of Arp 220W that is at least three times that found for the whole system of Arp 220. Such a line ratio indicates that the opacity of HCN 1-0 in the outflowing gas of Arp 220W is at least several times lower than that in other regions of Arp 220. Therefore, a lower conversion factor of HCN 1-0 luminosity to dense gas mass should be used in the outflowing gas than that used for the whole galaxy of Arp 220. Further sensitive observations of HCN/ H^{13}CN 2-1 or 1-0 with ALMA are necessary to constrain the opacity of HCN lines in the outflowing gas in Arp 220W.

Acknowledgements. We thank the anonymous referee for helpful comments to improve the manuscript. This work is supported by the National Natural Science Foundation of China grant 11988101, 11590783, and U1731237. This paper makes use of the following ALMA data: ADS/JAO.ALMA#2015.1.00702.S. ALMA is a partnership of ESO (representing its member states), NSF (USA) and NINS (Japan), together with NRC (Canada), MOST and ASIAA (Taiwan), and KASI (Republic of Korea), in cooperation with the Republic of Chile. The Joint ALMA Observatory is operated by ESO, AUI/NRAO and NAOJ.

References

- Aalto, S., Garcia-Burillo, S., Muller, S., et al. 2012, *A&A*, 537, A44. doi:10.1051/0004-6361/201117919
- Aalto, S., Garcia-Burillo, S., Muller, S., et al. 2015, *A&A*, 574, A85. doi:10.1051/0004-6361/201423987
- Barcos-Munoz, L. 2016, Ph.D. Thesis. doi:10.18130/V31S5F
- Barcos-Munoz, L., Aalto, S., Thompson, T. A., et al. 2018, *ApJ*, 853, L28. doi:10.3847/2041-8213/aaa28d
- Chisholm, J. & Matsushita, S. 2016, *ApJ*, 830, 72. doi:10.3847/0004-637X/830/2/72
- Cicone, C., Feruglio, C., Maiolino, R., et al. 2012, *A&A*, 543, A99. doi:10.1051/0004-6361/201218793
- Cicone, C., Maiolino, R., Sturm, E., et al. 2014, *A&A*, 562, A21. doi:10.1051/0004-6361/201322464
- Colzi, L., Fontani, F., Caselli, P., et al. 2018, *A&A*, 609, A129. doi:10.1051/0004-6361/201730576
- Feruglio, C., Maiolino, R., Piconcelli, E., et al. 2010, *A&A*, 518, L155. doi:10.1051/0004-6361/201015164
- Fischer, J., Sturm, E., González-Alfonso, E., et al. 2010, *A&A*, 518, L41. doi:10.1051/0004-6361/201014676
- Fluetsch, A., Maiolino, R., Carniani, S., et al. 2019, *MNRAS*, 483, 4586. doi:10.1093/mnras/sty3449
- Henkel, C., Asiri, H., Ao, Y., et al. 2014, *A&A*, 565, A3. doi:10.1051/0004-6361/201322962
- Henkel, C., Chin, Y.-N., Mauersberger, R., et al. 1998, *A&A*, 329, 443
- Li, F., Wang, J., Fang, M., et al. 2020, *MNRAS*, 494, 1095. doi:10.1093/mnras/staa676
- Lindberg, J. E., Aalto, S., Muller, S., et al. 2016, *A&A*, 587, A15. doi:10.1051/0004-6361/201527457
- Martín, S., Krips, M., Martín-Pintado, J., et al. 2011, *A&A*, 527, A36. doi:10.1051/0004-6361/201015855
- Michiyama, T., Iono, D., Sliwa, K., et al. 2018, *ApJ*, 868, 95. doi:10.3847/1538-4357/aae82a
- Padovani, M., Walmsley, C. M., Tafalla, M., et al. 2011, *A&A*, 534, A77. doi:10.1051/0004-6361/201117134

- Sturm, E., González-Alfonso, E., Velleux, S., et al. 2011, *ApJ*, 733, L16. doi:10.1088/2041-8205/733/1/L16
- van der Tak, F. F. S., Black, J. H., Schöier, F. L., et al. 2007, *A&A*, 468, 627. doi:10.1051/0004-6361:20066820
- Wang, J., Zhang, Z.-Y., Zhang, J., et al. 2016, *MNRAS*, 455, 3986. doi:10.1093/mnras/stv2580
- Wheeler, J., Glenn, J., Rangwala, N., et al. 2020, *ApJ*, 896, 43. doi:10.3847/1538-4357/ab8f32